crystals

MDPI

Article

Specific Structural Disorder in an Anion Layer and Its Influence on Conducting Properties of New Crystals of the (BEDT-TTF)$_4$A$^+$[M^{3+}(ox)$_3$]G Family, Where G Is 2-Halopyridine; M Is Cr, Ga; A$^+$ Is [K$_{0.8}$(H$_3$O)$_{0.2}$]$^+$

Tatiana G. Prokhorova [1,*], Eduard B. Yagubskii [1,*], Leokadiya V. Zorina [2,*], Sergey V. Simonov [2,3], Vladimir N. Zverev [2,3], Rimma P. Shibaeva [2] and Lev I. Buravov [1]

1 Institute of Problems of Chemical Physics of Russian Academy of Sciences, Chernogolovka 142432, Russia; buravov@icp.ac.ru
2 Institute of Solid State Physics of Russian Academy of Sciences, Chernogolovka 142432, Russia; simonovsv@rambler.ru (S.V.S.); zverev@issp.ac.ru (V.N.Z.); shibaeva@issp.ac.ru (R.P.S.)
3 Moscow Institute of Physics and Technology, Dolgoprudny 141701, Russia
* Correspondence: prokh@icp.ac.ru (T.G.P.); yagubski@icp.ac.ru (E.B.Y.); zorina@issp.ac.ru (L.V.Z.)

Received: 24 January 2018; Accepted: 8 February 2018; Published: 10 February 2018

Abstract: New crystals (**1–4**) of organic conductors based on the radical cation salts of the bis(ethylenedithio)tetrathiafulvalene (BEDT-TTF) with paramagnetic and diamagnetic tris(oxalato)metallate anions {A$^+$[M^{3+}(ox)$_3$]$^{3-}$G}$^{2-}$, where M is Cr, Ga; G is 2-chloropyridine, 2-bromopyridine; and A$^+$ is [K$_{0.8}$(H$_3$O)$_{0.2}$]$^+$ have been prepared and their crystal structure and transport properties were studied. All crystals belong to the monoclinic group of the (BEDT-TTF)$_4$A$^+$[M^{3+}(ox)$_3$]G family with β″-packing type of conducting BEDT-TTF layers. In contrast to the known superconducting crystals with M^{3+} = Fe^{3+} and G = 2-chloro- or 2-bromopyridine (T_c = 4.0–4.3 K), crystals with Cr^{3+} and Ga^{3+} ions exhibit metallic properties down to 0.5 K without superconducting transition. Upon cooling these crystals, the incommensurate superstructure appears, which has never been observed before in the numerous β″-salts of the family. In addition, orthorhombic (sp. group *Pbca*) semiconducting crystals α″-(BEDT-TTF)$_5$[Ga(ox)$_3$]·3.4·H$_2$O·0.6 EtOH (**5**) were obtained. It is a new compound in the family of BEDT-TTF crystals with tris(oxalato)metallate anions.

Keywords: molecular (super)conductors; superstructure; bifunctional compounds; radical cation salts; BEDT-TTF; tris(oxalato)metallate anions

1. Introduction

The great family of layered molecular conductors and superconductors based on radical cation salts of the bis(ethylenedithio)tetrathiafulvalene (BEDT-TTF) with supramolecular tris(oxalato)metallate anions includes compounds having a different stoichiometry, crystal structure, and various physical properties [1–33]. For example, the salt with the formula [BEDT-TTF]$_3$[M^{2+}M^{3+}(ox)$_3$], where M^{2+} is Mn^{2+} and M^{3+} is Cr^{3+} (3:1 salt), combine metallic conductivity and ferromagnetism in the same lattice [28]. The other group of salts with the stoichiometry 3:1 (BEDT-TTF)$_3$[NaM(ox)$_3$]G (where M = Cr, Al, and G = CH$_2$Cl$_2$, CH$_3$NO$_2$, DMF, CH$_3$CN, C$_2$H$_5$OH) includes semiconducting chiral crystals [29–32]. Recently, a 2:1 superconducting salt was synthesized, (BEDT-TTF)$_2$[(H$_2$O)(NH$_4$)$_2$Rh(ox)$_3$]·18-crown-6 [33].

The largest group of salts comprises paramagnetic (super)conductors (BEDT-TTF)$_4$A$^+$[M^{3+}(ox)$_3$]G (4:1 salts), where A$^+$ = K$^+$, NH^{4+}, Rb$^+$, H$_3$O$^+$, and M = Fe, Cr, Mn, Ru, Rh, Ga, Al, Co; and G is a neutral 'guest' solvent molecule [1–27]. The 4:1 crystals possess a great diversity of structural and conducting

properties. Several series of different polymorphs have been synthesized by varying A, M, and G. Almost all superconducting family crystals belong to this group.

In the structure of 4:1 crystals, the conducting layers of BEDT-TTF radical cations alternate with supramolecular anionic layers $\{A^+[M^{3+}(ox)_3]^{3-}G\}^{2-}$. The cationic and anionic layers are interconnected by hydrogen bonds that are formed between hydrogen atoms of terminal ethylene groups of BEDT-TTF and components of the complex anions.

Crystals of (BEDT-TTF)$_4$A$^+$[M^{3+}(ox)$_3$]G family can be divided into three series according to the type of their symmetry: monoclinic [1–17,19,21,23–27], orthorhombic [1,4,19,23,27], and triclinic [11,18–20,24,27]. The crystals of different series have different packing types of BEDT-TTF layers. Monoclinic crystals have the β″-packing type, according to the structural classification of the salts of BEDT-TTF and its analogues [34,35]. The β″-layers are composed of continuous stacks of radical cations, the planes of which are almost parallel and shifted with respect to the short axis of BEDT-TTF molecule. The interplanar distances in the stacks are considerably shortened in comparison with the normal van der Waals distances. There is a large number of shortened S$\cdots$S contacts between adjacent stacks in the layer. In the orthorhombic crystals with the 'pseudo-κ'-type of packing, the organic layer is formed by charged $[(BEDT\text{-}TTF)_2]^{2+}$ dimers surrounded by neutral [BEDT-TTF] molecules, which are perpendicular to the dimers. In the structure of triclinic crystals alternate conducting layers with two different packing types, α and β″ or α and 'pseudo-κ'. In the α-layer, the stacks of BEDT-TTF are inclined to one another.

The anionic layers have a honeycomb-like architecture: M^{3+} and A$^+$ cations linked by oxalate bridges alternate in vertices of the hexagonal network and form the hexagonal cavities in which neutral solvent molecules G are incorporated. The anion layers do not directly participate in conductivity, but the size and shape of G determine the crystal symmetry, the BEDT-TTF packing type and, hence, the conducting properties of crystals [1,3,17–20]. In contrast to G, the variation of M (keeping the G the same) in the composition of crystals does not lead to changes of the crystal structure, but affects the conducting properties. Thus, T_c of crystals with G = $PhNO_2$ gradually increases in a series of crystals with M = Cr, Fe, Ga (5.8 K, 6.2 K, 7.5 K, respectively). When G = Py, the crystals with Cr^{3+} and Fe^{3+} ions exhibit metallic behavior of resistance down to low helium temperatures, while crystals with Ga^{3+} ions experience a superconducting transition with $T_c < 2$ K. The crystals with G = PhBr (M^{3+} = Cr^{3+}, Mn^{3+}, Fe^{3+}, Ru^{3+}, Rh^{3+}) are superconductors with T_c = 2 K, 1 K, 4 K, 4 K, 2.5 K, respectively, while the salt with Ga^{3+} ions is a metal and does not transition to the superconducting state down to 0.4 K.

The group of crystals with halogen-containing solvents G is the most interesting among monoclinic crystals of the family, because the structural phase transitions from monoclinic to triclinic state, which were not found in other monoclinic crystals of the family, occur in many of these crystals (M^{3+} = Fe^{3+}) at low temperatures [21,22]. These transitions influence the ordering terminal ethylene groups in BEDT-TTF molecules [21,22,36] and, hence, the conducting properties of the crystals.

In our recent work [25] we reported on monoclinic crystals containing different isomers of halopyridines (HalPy, where Hal = Cl, Br) as guest solvents and Fe^{3+} as M^{3+}. It was shown that structural phase transitions at 180 K and the superconducting transition at 4.0–4.3 K take place in crystals with G = 2-ClPy and 2-BrPy, while neither phase transitions occur in crystals with G = 3-HalPy (Hal = Cl, Br). Here we report the synthesis, crystal structure, and transport properties of new monoclinic crystals β″-(BEDT-TTF)$_4$[$K_{0.8}(H_3O)_{0.2}$][M(ox)$_3$]G, where M/G = Cr/2-ClPy (**1**); Cr/2-BrPy (**2**); Ga/2-ClPy (**3**); Ga/2-BrPy (**4**). In addition, orthorhombic (sp. group *Pbca*) crystals α″-(BEDT-TTF)$_5$[Ga(ox)$_3$]·3.4·H_2O·0.6 EtOH (**5**) were obtained. Up to the present, crystals of this composition were not known in the family of BEDT-TTF salts with tris(oxalato)metallate anions.

2. Materials and Methods

BEDT-TTF, 1,2,4-trichlorobenzene, 2-chloropyridine, 3-chloropyridine, 2-bromopyridine, and $K_3[Cr(ox)_3]\cdot 3H_2O$ were used as received (SIGMA-ALDRICH CHEMIE, GmbH, Steinheim, Germany);

18-crown-6 (the same firm) was purified by recrystallization from acetonitrile and dried in vacuum at 30 °C over P_2O_5; and $K_3[Ga(ox)_3]\cdot 5H_2O$ was synthesized according to the procedure described in [37].

2.1. Synthesis

Electrocrystallization of the charge transfer salts was performed in conventional two-compartment H-shaped cells with Pt wire electrodes at constant current and temperature (25 °C). BEDT-TTF, the supporting electrolyte, 18-crown-6, and a solvent (or a mixture of solvents) was placed in the cathode compartment of the cell. The obtained solution was distributed between the two compartments of the cell. The exact conditions for the synthesis of each salt are described below.

2.1.1. β″-(BEDT-TTF)$_4$[$K_{0.8}(H_3O)_{0.2}$][Cr(ox)$_3$]·(2-ClPy) (**1**)

24 mg of BEDT-TTF, 170 mg of $K_3[Cr(ox)3]\cdot 3H_2O$, 220 mg of 18-crown-6 and the mixture of 2-ClPy (30 mL) with 1,2,4-trichlorobenzene (4 mL) and 96% EtOH (3.5 mL) were used. J = 0.97 μA. Several crystals in the form of prisms were collected from the anode after 3 weeks.

2.1.2. β″-(BEDT-TTF)$_4$[$K_{0.8}(H_3O)_{0.2}$][Cr(ox)$_3$]·(2-BrPy) (**2**)

25 mg of BEDT-TTF, 50 mg of $K_3[Cr(ox)_3]\cdot 3H_2O$, 200 mg of 18-crown-6 and the mixture of 2-BrPy (8 mL) with 1,2,4-triclorobenzene (10 mL) and 96% ethanol (3.5 mL) were used. J = 0.95 μA. Several crystals in the form of thick plates were collected from the anode after 10 days.

2.1.3. β″-(BEDT-TTF)$_4$[$K_{0.8}(H_3O)_{0.2}$][Ga(ox)$_3$]·(2-ClPy) (**3**) and α″-(BEDT-TTF)$_5$]·3.4·H_2O·0.6 EtOH (**5**)

(a) 11 mg of BEDT-TTF, 300 mg of $K_3[Ga(ox)_3]\cdot 5H_2O$, 300 mg of 18-crown-6 and the mixture of 2-ClPy (20 mL) with 1,2,4-trichlorobenzene (10 mL) and 96% ethanol (3.5 mL) were used. J = 0.9 μA. Many shining black α″-crystals (**5**) in the form of thin plates and a few small β″-crystals (**3**) were collected from the anode after 14 days. After removing these crystals, β″-crystals (**3**) started to grow and a few of these crystals in the form of elongated plates were collected after 10 days.

(b) 25 mg of BEDT-TTF, 300 mg of $K_3[Ga(ox)_3]\cdot 5H_2O$, 300 mg of 18-krown-6; 20 mL of 2-ClPy, 10 mL of 1,2,4-trichlorobenzene, 3.5 mL of 96% ethanol were used. J = 0.95 μA. A lot of α″-crystals (**5**) in the form of thick plates were obtained after 15 days.

(c) 15 mg of BEDT-TTF, 350 mg of $K_3[Ga(ox)_3]\cdot 5H_2O$, 700 mg of 18-krown-6; 20 mL of 3-ClPy, 10 mL of 1,2,4-trichlorobenzene, 2 mL of 96% ethanol were used. J = 0.95 μA. A few large thick α″-crystals (**5**) were obtained after 10 days.

2.1.4. β″-(BEDT-TTF)$_4$[$K_{0.8}(H_3O)_{0.2}$][Ga(ox)$_3$]·(2-BrPy) (**4**)

15 mg of BEDT-TTF, 150 mg of $K_3[Ga(ox)_3]\cdot 5H_2O$, 450 mg of 18-krown-6; 10 mL of 1,2,4-trichlorobenzene, 20 mL of 2-BrPy, 3 mL of 96% ethanol were used. J = 0.95 μA. A few crystals (**4**) in the form of thick plates were collected from the anode after three weeks.

2.2. Crystal Structure

Single crystal X-ray diffraction experiments were carried out on an Oxford Diffraction Gemini-R CCD diffractometer (λ(MoKα) = 0.71073 Å, graphite monochromator, ω-scan mode). Data reduction with empirical absorption correction of experimental intensities (Scale3AbsPack program) was made with the CrysAlisPro software [38]. The structures were solved by the direct method and refined by the full-matrix least-squares technique against F^2 in an anisotropic approximation for all non-hydrogen atoms using the SHELX-2016 software package [39]. H-atoms were placed in idealized positions and refined using a riding model with U_{iso}(H) depending on U_{eq} of the parent C/O atom. Hydrogen atoms in water molecules (structure **5**) were localized from the Fourier synthesis of the electron density and refined with $U_{iso}(H) = 1.5U_{eq}(O)$. Hydrogen atoms in the $(H_3O)^+$ cations were not localized, but added into the chemical formula of **1**–**4**. Selected crystallographic data and refinement parameters are given

in Table 1. The full data of studies are available at the Cambridge Crystallographic Data Centre via www.ccdc.cam.ac.uk/data_request/cif (CCDC 1818020-1818024).

Table 1. Crystal structure and refinement data.

	1	2	3	4	5
Chemical formula	$C_{51}H_{36.6}ClCrK_{0.8}NO_{12.2}S_{32}$	$C_{51}H_{36.6}BrCrK_{0.8}NO_{12.2}S_{32}$	$C_{51}H_{36.6}ClGaK_{0.8}NO_{12.2}S_{32}$	$C_{51}H_{36.6}BrGaK_{0.8}NO_{12.2}S_{32}$	$C_{56.6}H_{48.6}GaO_{15.7}S_{40}$
Formula weight	2003.26	2047.72	2020.98	2065.44	919.70
Temperature (K)	270	295	295	295	120
Cell setting	monoclinic	monoclinic	monoclinic	monoclinic	orthorhombic
Space group, *Z*	*C*2/*c*, 4	*C*2/*c*, 4	*C*2/*c*, 4	*C*2/*c*, 4	*Pbca*, 8
a (Å)	10.2791(6)	10.2971(2)	10.27760(10)	10.27515(15)	22.0871(4)
b (Å)	20.0020(9)	20.0382(5)	19.9066(3)	20.0182(4)	21.0853(4)
c (Å)	35.4485(15)	35.4621(8)	35.5504(5)	35.5972(5)	35.6286(7)
α (°)	90	90	90	90	90
β (°)	92.948(4)	93.2943(19)	92.9970(10)	93.2026(13)	90
γ (°)	90	90	90	90	90
Cell volume (Å^3)	7278.7(6)	7305.0(3)	7263.4(2)	7310.5(2)	16592.7(5)
Crystal size (mm)	0.53 × 0.25 × 0.12	0.35 × 0.34 × 0.21	0.42 × 0.30 × 0.15	0.61 × 0.27 × 0.12	0.83 × 0.18 × 0.03
ρ (Mg/m^3)	1.828	1.862	1.848	1.877	1.867
μ, cm^{-1}	12.17	17.23	14.41	19.42	14.02
Refls collected/unique/observed with $I > 2\sigma(I)$	37,634/10,476/8631	17,952/9860/8119	17,486/9629/8063	33,996/10,184/8082	64,803/23,232/17,944
R_{int}	0.0291	0.0154	0.0285	0.0187	0.0263
θ_{max} (°)	31.12	30.36	29.93	30.60	30.72
Parameters refined	608	606	612	606	1076
Final R_1(obs), wR_2 (all)	0.0463, 0.1217	0.0637, 0.1962	0.0445, 0.1203	0.0535, 0.1586	0.0425, 0.1101
Goodness-of-fit	1.004	1.004	1.005	1.003	1.005
Residual electron density (e Å^{-3})	1.188/–0.695	1.722/–1.937	1.039/–0.728	2.068/–1.174	2.767/–1.492
CCDC reference	1818020	1818021	1818022	1818023	1818024

2.3. Conducting Properties

The temperature dependencies of the electrical resistance of single crystals was measured using a four-probe technique by a lock-in detector at 20 Hz alternating current, J = 1 μA. Two contacts were attached to each of two opposite sample surfaces with conducting graphite paste. In the experiment we have measured the out-of-plane resistance $R_\perp$ with the current running perpendicular to conducting layers. The magnetotransport measurements at low temperatures down to 0.5 K were carried out in a cryostat with a superconducting solenoid, which generated a magnetic field of up to 17 T.

3. Results and Discussion

3.1. Synthesis

It was known that crystals of orthorhombic 'pseudo-κ'-phases are obtained together with monoclinic β″-crystals in some cases [1,19] (concomitant polymorphism). In this work, we have shown that the use of 2-ClPy as a guest solvents and $[Ga(ox)_3]^{3-}$ as a counterion leads to the formation of both β″-(BEDT-TTF)$_4$[$K_{0.8}(H_3O)_{0.2}$][$Ga(ox)_3$]·2-ClPy (**3**) and α″-(BEDT-TTF)$_5$[$Ga(ox)_3$]·3.4·H_2O·0.6 EtOH (**5**) (sp. group *Pbca*) crystals in the same synthesis. Crystal **5** was not previously found in this family. It should be noted that β″ crystals start to grow much later then α″ crystals. When G = 3-ClPy, only α″ crystals are formed (see Section 2.1.3 (c)).

3.2. Crystal Structure

3.2.1. β″-(BEDT-TTF)$_4$[$K_{0.8}(H_3O)_{0.2}$][$M(ox)_3$]·2-HalPy, where M/Hal = Cr/Cl (**1**), Cr/Br (**2**), Ga/Cl (**3**) and Ga/Br (**4**)

Compounds **1**–**4** crystallize in the monoclinic *C*2/*c* space group with one half of the formula unit in the crystallographic asymmetric unit (Figure 1). They are isostructural to the series of β″ salts of the

(BEDT-TTF)$_4$A$^+$[M^{3+}(ox)$_3$]·G family, but have a specific disorder in the anion part which is described in the caption to Figure 1.

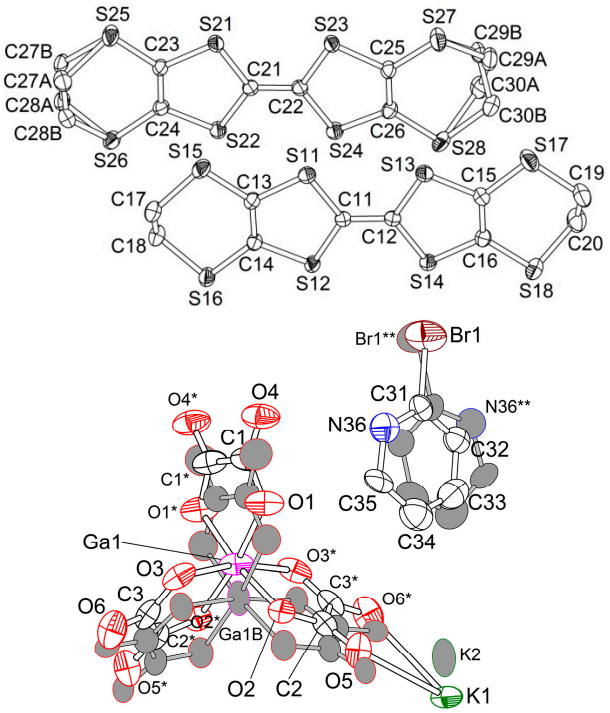

Figure 1. Asymmetric unit in **4** (30% level of thermal ellipsoids). Symmetry codes: (*) $(1 - x, y, 1.5 - z)$, (**) $(-x, y, 1.5 - z)$. Anion $[Ga(ox)_3]^{3-}$ and cation K^+ are in the special positions on a two-fold axis, and the solvent is in the general position near a two-fold axis. The K1 site is occupied by a mixture of K^+/H_3O^+ cations in a ratio of 0.60/0.20 in **1** and **4**, 0.56/0.20 in **2** and 0.68/0.20 in **3**. There is a second independent position of the anion and K^+ cation (grey color) with occupancy of Cr1B(Ga1B)/K2 sites of 0.25/0.20 in **1** and **4**, 0.32/0.24 in **2** and 0.12/0.12 in **3**.

The crystal structure consists of radical cation and anion layers alternating along the *c*-axis of the lattice (Figure 2a). The radical cation layer has a β”-type of molecular packing (Figure 2b). Two independent BEDT-TTF radical cations, A and B, form stacks in . . . -(ABBA)-(ABBA)- . . . sequence with both longitudinal and transversal shift of the adjacent BEDT-TTF within the (ABBA) tetrad and only transversal displacement between the tetrads (Figure 2c). Intermolecular separations along the stack are 3.54(1) (A···A), 3.58(4) (A···B), and 3.65(1) Å (B···B) in **1**–**4**. The radical cation A is fully ordered at room temperature, whereas both terminal ethylene groups of B are disordered in two sites with the occupation ratio of 0.67/0.33 and 0.52/0.48 in **1**, 0.67/0.33 and 0.62/0.38 in **2**, 0.63/0.37 and 0.57/0.43 in **3**, 0.70/0.30 and 0.60/0.40 in **4**. Analysis of bond length distributions in BEDT-TTF radical cations [40] gives equal charge on A and B of 0.5+ in accordance with stoichiometry of the compound. The shortest S···S contacts in the conducting layer are side-by-side ones between BEDT-TTF from adjacent stacks in the range of 3.334–3.570(1) Å (dashed bonds in Figure 2b).

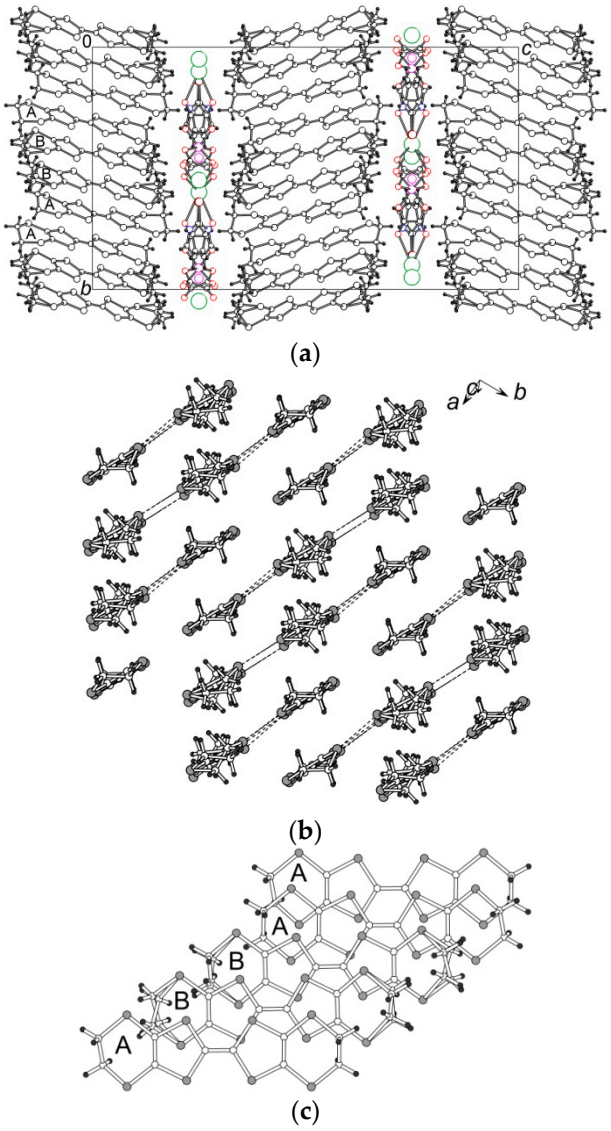

Figure 2. (**a**) Projection of the structure of **4** along *a* (the minor part of the $[Ga(ox)_3]^{3-}$ anion is omitted, except for Ga1B and K2 atoms); (**b**) view of the radical cation β″-layer along the long axis of BEDT-TTF with short intermolecular S···S contacts < 3.6 Å (dashed lines); and (**c**) overlap modes within the stack.

The anion layer in **1**–**4** shows the additional positional disorder of the $[M^{3+}(ox)_3]^{3-}$ anion and small monovalent A^+ cation. Such a type of disorder has never been observed before in the numerous β″-salts of the (BEDT-TTF)$A^+[M^{3+}(ox)_3]$·G family. It is roughly described in the room temperature structures of **1**–**4** as a shift of the anion unit and A^+ cations along the two-fold monoclinic axis by about 1 Å, the shift for M^{3+} and A^+ centers being in opposite directions (Figures 1 and 3). Maximal occupation of the second position is observed in **2**: 0.32 for Cr1B and 0.24 for K2. The amount of the second position in **3** (0.12 for both Ga1B and K2) is about two times less than in **1** and **4** (0.25 for Cr1B or Ga1B and 0.20 for K2). Molecules with major occupancy form typical β″-salts of the family's honeycomb-like packing with guest solvent molecules filling the hexagonal cavities of the anion layer (Figure 3). Each anion layer contains only one enantiomer of the chiral anion, but th whole crystal is racemic due to alternation of the enantiopure layers of different chirality along *c*. Contacts between K1 site occupied by mixture of K^+/H_3O^+ cations and oxygen atoms of surrounding oxalate groups are in the range of 2.87–3.08 Å in **1**, 2.88–3.13 Å in **2**, 2.85–2.97 Å in **3** and 2.91–3.11 Å in **4** (they are shown by red dashed

lines in Figure 3). Upon cooling crystals **1**–**4**, the incommensurate superstructure appears, which is apparently connected with specific ordering in the anion layer and will be described elsewhere.

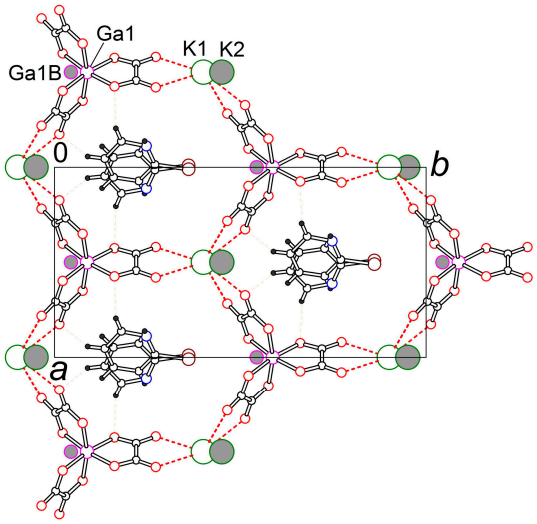

Figure 3. Anion layer in **4**. K2 and Ga1B atoms of minor occupancy are shown in grey; oxalate groups of minor part of the anions are omitted for clarity.

3.2.2. α″-(BEDT-TTF)$_5$[Ga(ox)$_3$]·3.4·H$_2$O·0.6 EtOH (**5**)

Compound **5** crystallizes in the orthorhombic *Pbca* space group. The asymmetric unit contains five independent BEDT-TTF molecules, one $[Ga(ox)_3]^{3-}$ anion, four H_2O molecules, two of which have an occupancy of 0.7 and are mixed in the same site with 0.3 EtOH molecule (Figure 4).

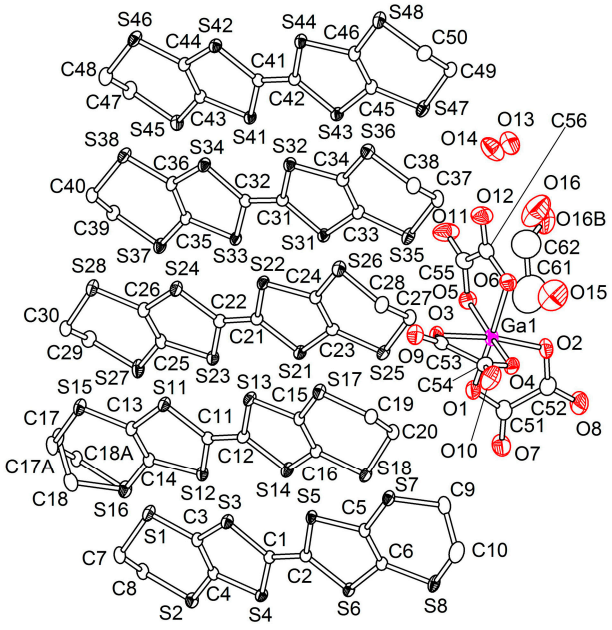

Figure 4. Asymmetric unit in **5** (50% level of thermal ellipsoids).

The structure of **5** is composed of radical cation and anion layers alternating along the *c*-axis (Figure 5). Water and ethanol molecules are included into the anion layer. According to the X-ray data, neither 2-chloropyridine solvent nor K^+ cation is found in the composition of **5**.

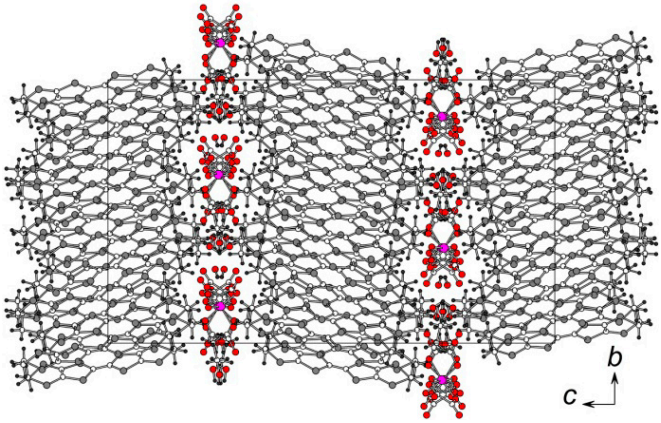

Figure 5. Projection of the structure **5** along a.

The conducting layer has an α″-type of molecular packing (Figure 6a). It consists of the stacks with a . . . (BCDEA)-(BCDEA) . . . repeating sequence of BEDT-TTF radical cations (Figure 6b). In the pair of neighbor stacks (1 and 2 in Figure 6a) the molecular planes are near parallel to each other (angles 0.48–2.85(2)°) whereas all the molecules in the next pair of stacks (3, 4) are tilted relative to the molecules from the first pair by an angle of 53(2)°. Radical cations inside the pentad (BCDEA) overlap with a pure transversal shift of adjacent units; longitudinal displacement is added only between the pentads in A···B interaction (Figure 6c). Intrastack interplanar distances are shown in Figure 6b. The maximal interplanar separation is observed between the pentads in the A···B pair. Only one ethylene group (C17–C18) in BEDT-TTF B is disordered at 120 K between two orientations of 0.4/0.6 occupancy. The ethylene groups of molecules B (major part), C, D, and E are eclipsed and the sole BEDT-TTF A has a staggered conformation. The overall charge on five BEDT-TTF units is +3 according to the formula of the salt. Calculations of the charge state using the empirical formula for BEDT-TTF compounds [40] show a non-uniform charge distribution along the stack with values of +0.62, +0.37, +0.76, +0.83, and +0.53 for A, B, C, D, abd E radical cations, respectively, which gives a total charge of +3.11, which is in good agreement with the stoichiometric +3 value. There are many interstack S . . . S contacts less than sum of van der Waals radii (3.6 Å) shown by dashed lines in Figure 6a, but no intrastack one.

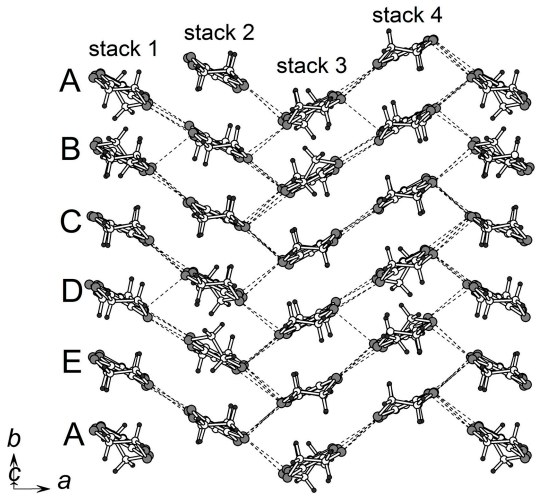

(**a**)

Figure 6. *Cont.*

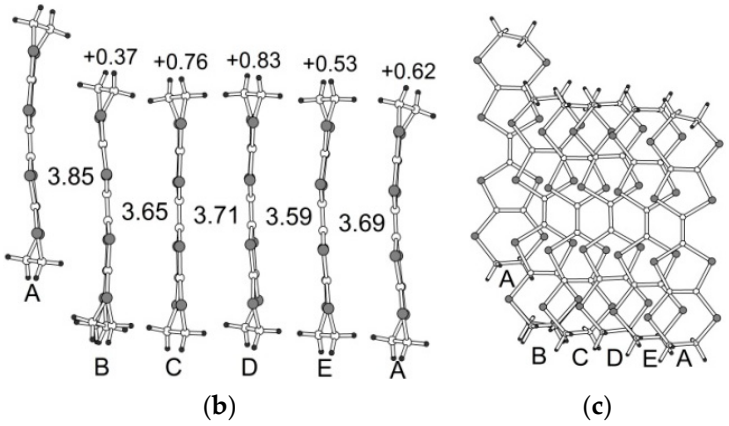

Figure 6. (**a**) View of the radical cation layer of α″-type in **5** along the long molecular axis. Short S···S contacts < 3.6 Å are shown by dashed lines; (**b**) side view of the stack with interplanar separations (in Å) and calculated charges of BEDT-TTF; and (**c**) overlap modes within the stack.

The anion layer in **5** consists of $[Ga(ox)_3]^{3-}$ anions interacting by hydrogen bonding through water molecules (Figure 7).

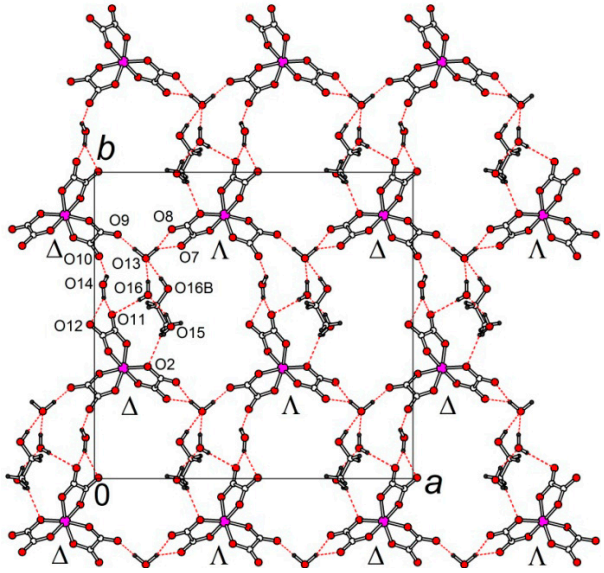

Figure 7. The anion layer in **5**. O-H . . . O hydrogen bonds are shown by red dashed lines.

Right-handed Δ and left-handed Λ isomers of the chiral anion alternate along the *a* direction. Water molecules O(13) connect the different enantiomers of the anion along *a* and O(14) join similar enantiomers along *b*, resulting to a network of tilted parallelograms having Ga atoms at the vertices. Additional disordered water and ethanol molecules are located in the free cavity near one side of parallelogram and form hydrogen bonds with the anion and water molecule O(13).

α″-packing of the radical cation layer has been found before in one of BEDT-TTF salts with tris(oxalato)metallate anions α″-(BEDT-TTF)$_4$H$_2$OLi[Fe(ox)$_3$] solvent [41]. This salt differs from **5** by a cation to anion ratio (4:1 vs. 5:1), as well as the anion layer structure and possesses a semiconductor behavior with activation energy of 0.080 eV and a room temperature resistivity ρ_{RT} of 2.41 Ohm cm. Another salt with the same as in **5** composition of 5:1 is known among BEDT-TTF conductors with $[M(ox)_3]^{3-}$ anions: (BEDT-TTF)$_5$[Fe(ox)$_3$]·(H$_2$O)$_2$·CH$_2$Cl$_2$ [42]. It differs from **5** by both symmetry and crystal structure. The anion layer is also build of parallelograms, but they are arranged in another way

than in **5** because each layer is chiral. The conducting layer has close to β″-type of BEDT-TTF-packing and the crystal is a paramagnetic semiconductor.

3.3. Conducting Properties

Temperature dependencies of the out-of-plane resistance $R_{\perp}$ for samples **1**–**4** are presented in Figure 8. One can see that all the samples show the metallic behavior and the R(T) dependencies for all samples look very similar. Unlike to these samples, the sample **5** demonstrates the dielectric behavior (see Figure 9) with the activation energy 71 meV as it is seen from the inset in Figure 9. For the samples **1**–**4** at T $\leq$ 10 K the derivative of the R(T) dependencies changes the sign: the resistance starts to grow when the temperature decreases. This growth is more pronounced for sample **3**, and is comparatively small for sample **2**. This growth is shown in the inset in Figure 8 for samples **1** and **4**, where the sample resistance R(T)/R(290K) is plotted as function of T in the logarithmic scale.

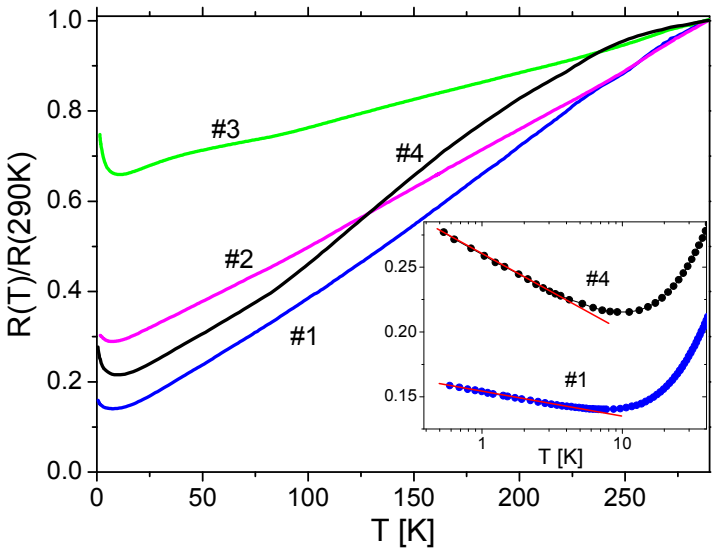

Figure 8. The temperature dependencies of the out-of-plane resistance $R_{\perp}(T)$ for crystals **1**–**4**. The R(290K) values are 287 Ohm, 3.77 kOhm, 2.52 kOhm, and 427 Ohm, respectively. The inset shows the resistance R(T)/R(290K) as function of T in the logarithmic scale for the samples **1** and **4**.

We have made an attempt to find the Shubnikov-de Haas oscillations in the magnetoresistance for our samples at T = 0.5 K in magnetic fields up to 17 T, but, unfortunately, without success.

The growth of the sample resistance at low temperatures T $\leq$ 10 K could be attributed to the following mechanisms: (i) by the localization effects due to the quantum interference of the carriers at the presence of elastic scattering processes [43] or (ii) by the scattering of the carriers on the magnetic impurities due to the so-called Kondo effect [44]. Both of these two effects lead to the logarithmic temperature dependence for the sample resistance in quasi two-dimensional systems. In our samples the magnetic impurities (Cr) are only in samples **1** and **2**. The fact that we observe the low-temperature resistance growth in all our samples means that we deal with the localization effects due to the quantum interference of the carriers [43]. This effect is characteristic for the systems with disorder which, in our case, seem to be the reason not only for the quantum localization effects on R(T) dependence, but also for the absence of the Shubnikov-de Haas oscillations, because the high scattering rate leads to the broadening of the Landau levels and to the smearing of the quantum oscillations. Most likely, the absence of Shubnikov-de Haas oscillations is associated with the specific disorder in the anion layer (see Section 2.2) which is observed in the β″-(BEDT-TTF)$A^{+}[M^{3+}(ox)_3]\cdot G$ crystals for the first time and causes appearance of incommensurate structural modulation at low temperatures. The incommensurability in the anion layer creates the perturbative potential for the

carriers in the conducting layer, which acts as disorder for the carriers moving in the periodical crystal lattice. This disorder certianly leads to additional scattering and to the broadening of the Landau levels.

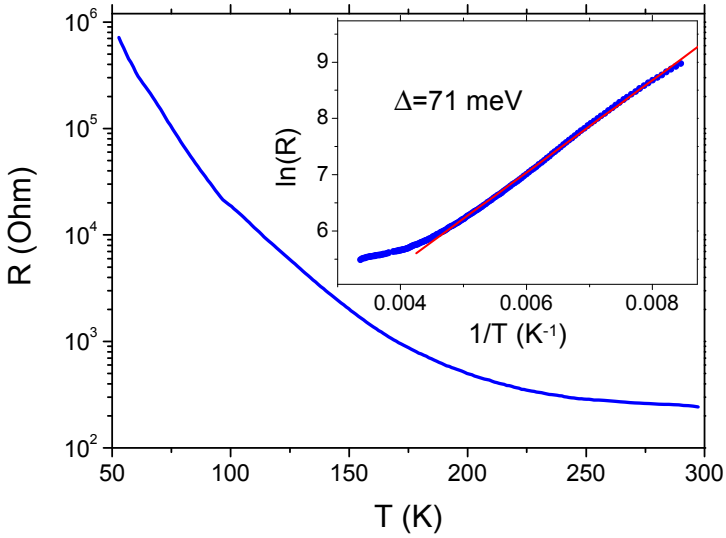

Figure 9. The temperature dependencies of the out-of-plane resistance $R_{\perp}(T)$ for crystal **5**. The inset demonstrates the activation behavior of the sample resistance at T < 215 K.

4. Conclusions

Four new radical cation salts of the family of layered molecular (super)conductors based on bis(ethylenedithio)tetrathiafulvalene (BEDT-TTF) with tris(oxalato)metallate anions $(BEDT\text{-}TTF)_4\{A^+[M^{3+}(ox)_3]G\}$, where M/G = Cr/2-ClPy (**1**); Cr/2-BrPy (**2**); Ga/2-ClPy (**3**), Ga/2-BrPy (**4**); and $A^+ = [K_{0.8}(H_3O)_{0.2}]^+$ were obtained. These salts belong to the monoclinic group of the family with a β″-packing type of radical cation layers. The conducting and structural properties of β″-crystals strongly depend on the size, shape, and chemical nature of the guest solvent molecule G. In some crystals with G = halobenzenes and M = Fe, the structural phase transition from the monoclinic to the triclinic state was found upon lowering the temperature [21,22,36]. In our recent work we showed that the same transition also exists in superconducting Fe crystals with G = 2-ClPy and 2-BrPy (T_c = 4.0 K and 4.3 K, respectively) [25]. These structural transitions arise from noticeable positional shifts of all components of the complex anion, giving rise to two nonequivalent organic β″ layers and the partial ordering of the ethylene groups of BEDT-TTF molecules. In the present paper, we found that the change of the Fe^{3+} ion by Cr^{3+} or Ga^{3+} ions, as well as the $(H_3O)^+$ cation by $[K_{0.8}(H_3O)_{0.2}]^+$ in one of the compositions of $\beta''\text{-}(BEDT\text{-}TTF)_4\{A^+[M^{3+}(ox)_3](2\text{-}HalPy)\}$ crystals leads to the appearance of a specific disorder in anionic layers associated with the position disorder of the $[M^{3+}(ox)_3]^{3-}$ anion and the small monovalent A^+ cation. Such a type of disorder has never been observed before in the numerous β″-salts of the $(BEDT\text{-}TTF)A^+[M^{3+}(ox)_3]\cdot G$ family. Unlike the crystals with Fe^{3+} ions, the crystals with Cr^{3+} and Ga^{3+} ions do not exhibit a superconducting transition down to 0.5 K. At T $\leq$ 10 K, they demonstrate a weak growth of resistance. The fact that we observed the low-temperature resistance growth in all our samples (with magnetic Cr^{3+} and non-magnetic Ga^{3+} ions) means that we experienced the localization effects due to the quantum interference of the carriers [43]. This effect is characteristic for the systems with disorder which, in our case, seems to be the reason not only for the quantum localization effects on R(T) dependencies, but also for the absence of the Shubnikov-de Haas oscillations, because the high scattering rate leads to the broadening of the Landau levels and to the smearing of the quantum oscillations.

Acknowledgments: The work was carried out within the state assignments for ISSP RAS and for IPCP RAS, theme No. 0089-2014-0026, and partially supported by the Russian Foundation for Basic Research (RFBR), grant No. 18-02-00280.

Author Contributions: T.G.P., E.B.Y. conceived, designed, and performed the chemical experiments and also wrote the Abstract, Introduction, Synthesis, and Conclusions; L.V.Z., S.V.S., and R.P.S. performed the X-ray experiments, analyzed the X-ray data, and described them (the section titled "Crystal Structure"); and V.N.Z. and L.I.B. performed the conductivity measurement on the crystals and wrote the section titled "Conducting Properties".

Conflicts of Interest: The authors declare no conflict of interest. The founding sponsors had no role in the design of the study; in the collection, analyses, or interpretation of data; in the writing of the manuscript; or in the decision to publish the results.

References

1. Kurmoo, M.; Graham, A.W.; Day, P.; Coles, S.J.; Hursthouse, M.B.; Caufield, J.L.; Singleton, J.; Pratt, F.L.; Hayes, W.; Ducasse, L.; et al. Superconducting and Semiconducting Magnetic Charge Transfer Salts: (BEDT-TTF)$_4$AFe(C_2O_4)$_3$ C_6H_5CN A = H_2O, K, NH_4. *J. Am. Chem. Soc.* **1995**, *117*, 12209–12217. [CrossRef]
2. Martin, L.; Turner, S.S.; Day, P.; Mabbs, F.E.; McInnes, J.L. New molecular superconductor containing paramagnetic chromium (III) ions. *Chem. Commun.* **1997**, *15*, 1367–1368. [CrossRef]
3. Turner, S.S.; Day, P.; Abdul Malik, K.M.; Hursthouse, M.B.; Teat, S.J.; MacLean, E.J.; Martin, L.; French, S.A. Effect of Included Solvent Molecules on the Physical Properties of the Paramagnetic Charge Transfer Salts β''-(BEDT-TTF)$_4$[(H_3O)Fe(C_2O_4)$_3$]·Solvent (BEDT-TTF = Bis(ethylenedithio)tetrathiafilvalene). *Inorg. Chem.* **1999**, *38*, 3543–3549. [CrossRef] [PubMed]
4. Martin, L.; Turner, S.S.; Day, P.; Guionneau, P.; Howard, J.A.K.; Hibbs, D.E.; Light, M.E.; Hursthouse, M.B.; Uruichi, M.; Yakushi, K. Crystal Chemistry and Physical Properties of Superconducting and Semiconducting Charge Transfer Salts of the Type (BEDT-TTF)$_4$[A^IM^{III}(C_2O_4)$_3$]·PhCN (A^I = H_3O, NH_4, K; M^{III} = Cr, Fe, Co, Al; BEDT-TTF = Bis(ethylenedithio)tetrathiafulvalene). *Inorg. Chem.* **2001**, *40*, 1363–1371. [CrossRef] [PubMed]
5. Rashid, S.; Turner, S.S.; Le Pevelen, D.; Day, P.; Light, M.E.; Hursthouse, M.B.; Firth, S.; Clark, R.J.H. β''-BEDT-TTF)$_4$[(H_3O)Cr(C_2O_4)$_3$]CH_2Cl_2: Effect of Included Solvent on the Structure and Properties of a Conducting Molecular Charge-Transfer Salt. *Inorg. Chem.* **2001**, *40*, 5304–5306. [CrossRef] [PubMed]
6. Rashid, S.; Turner, S.S.; Day, P.; Howard, J.A.K.; Guionneau, P.; McInnes, E.J.L.; Mabbs, F.E.; Clark, R.J.H.; Firth, S.; Biggse, T. New superconducting charge-transfer salts (BEDTTTF)$_4$[AM(C_2O_4)3]$C_6H_5NO_2$(A = H_3O or NH_4, M = Cr or Fe, BEDT-TTF = bis(ethylenedithio)tetrathiafulvalene. Novel charge transfer salts of BEDT-TTF with metal oxalate counterions. *J. Mater. Chem.* **2001**, *11*, 2095–2101. [CrossRef]
7. Rashid, S.S.; Turner, P.; Day, M.E.; Light, M.B.; Hursthouse, P. Guionneau. *Synth. Met.* **2001**, *120*, 985–986. [CrossRef]
8. Akutsu, H.; Akutsu-Sato, A.; Turner, S.S.; Le Pevelen, D.; Day, P.; Laukhin, V.; Klehe, A.-K.; Singleton, J.; Tocher, D.A.; Probert, M.R.; et al. Effect of Included Guest Molecules on the Normal State Conductivity and Superconductivity of β''-(ET)$_4$[(H_3O)Ga(C_2O_4)$_3$]G (G = Pyridine, Nitrobenzene). *J. Am. Chem. Soc.* **2002**, *124*, 12430–12431. [CrossRef] [PubMed]
9. Prokhorova, T.G.; Khasanov, S.S.; Zorina, L.V.; Buravov, L.I.; Tkacheva, V.A.; Baskakov, A.A.; Morgunov, R.B.; Gener, M.; Canadell, E.; Shibaeva, R.P.; et al. Molecular Metals Based on BEDT-TTF Radical Cation Salts with Magnetic Metal Oxalates as Counterions: β''-(BEDT-TTF)$_4$A[M(C_2O_4)$_3$]DMF (A = K^+, NH_4^+; M = Fe^{III}, Cr^{III}). *Adv. Funct. Mater.* **2003**, *13*, 403–411. [CrossRef]
10. Coldea, A.I.; Bangura, A.F.; Singleton, J.; Ardavan, A.; Akutsu-Sato, A.; Akutsu, H.; Turner, S.S.; Day, P. Fermi-surface topology and the effects of intrinsic disorder in a class of charge-transfer salts containing magnetic ions: β''-(BEDT-TTF)$_4$[(H_3O)M(C_2O_4)$_3$]Y (M = Ga, Cr, Fe; Y = C_5H_5N. *Phys. Rev. B* **2004**, *69*, 085112. [CrossRef]
11. Akutsu, H.; Akutsu-Sato, A.; Turner, S.S.; Day, P.; Canadell, E.; Firth, S.; Clark, R.J.N.; Yamada, J.; Nakatsuji, S. Superstructures of donor packing arrangements in a series of molecular charge transfer salts. *Chem. Commun.* **2004**, *1*, 18–19. [CrossRef] [PubMed]
12. Audouard, A.; Laukhin, V.N.; Brossard, L.; Prokhorova, T.G.; Yagubskii, E.B.; Canadell, E. Combination frequencies of magnetic oscillations in β''-(BEDT-TTF)$_4$(NH_4)[(Fe(C_2O_4)$_3$]DMF. *Phys. Rev. B* **2004**, *69*, 144523. [CrossRef]

13. Akutsu-Saito, A.; Kobayashi, A.; Mori, T.; Akutsu, H.; Yamada, J.; Nakatsuji, S.; Turner, S.S.; Day, P.; Tocher, D.A.; Light, M.E.; et al. Structures and Physical Properties of New β″-BEDT-TTF Tris-Oxalatometallate (III) Salts Containing Chlorobenzene and Halomethane Guest Molecules. *Synth. Met.* **2005**, *152*, 373–376. [CrossRef]
14. Coronado, E.; Curelli, S.; Giménez-Saiz, C.; Gómez-García, C.J. New magnetic conductors and superconductors based on BEDT-TTF and BEDS-TTF. *Synth. Met.* **2005**, *154*, 245–248. [CrossRef]
15. Coronado, E.; Curelli, S.; Giménez-Saiz, C.; Gómez-García, C.J. A novel paramagnetic molecular superconductor formed by bis(ethylenedithio)tetrathiafulvalene, tris(oxalato)ferrate(III) anions and bromobenzene as guest molecule: $(ET)_4[(H_3O)Fe(C_2O_4)_3]C_6H_5Br$. *J. Mater. Chem.* **2005**, *15*, 1429–1436. [CrossRef]
16. Akutsu-Sato, A.; Akutsu, H.; Yamada, J.; Nakatsuji, S.; Turner, S.S.; Day, P. Suppression of superconductivity in a molecular charge transfer salt by changing quest molecule: β''-$(BEDT\text{-}TTF)_4[(H_3O)Fe(C_2O_4)_3](C_6H_5CN)_x(C_5H_5N)_{1-x}$. *J. Mater. Chem.* **2007**, *17*, 2497–2499. [CrossRef]
17. Zorina, L.V.; Prokhorova, T.G.; Simonov, S.V.; Khasanov, S.S.; Shibaeva, R.P.; Manakov, A.I.; Zverev, V.N.; Buravov, L.I.; Yagubskii, E.B. Structure and Magnetotransport Properties of the New Quasi-Two-Dimensional Molecular Metal β''-$(BEDT\text{–}TFF)_4H_3O[Fe(C_2O_4)_3]C_6H_4Cl_2$. *J. Exp. Theor. Phys.* **2008**, *106*, 347–354. [CrossRef]
18. Martin, L.; Day, P.; Akutsu, H.; Yamada, J.; Nakatsuji, S.; Clegg, W.; Harrington, R.W.; Horton, P.N.; Hursthouse, M.B.; McMillan, P.; et al. Metallic molecular crystals containing chiral or racemic guest molecules. *CrystEngComm* **2007**, *9*, 865–867. [CrossRef]
19. Prokhorova, T.G.; Buravov, L.I.; Yagubskii, E.B.; Zorina, L.V.; Khasanov, S.S.; Simonov, S.V.; Shibaeva, R.P.; Korobenko, A.V.; Zverev, V.N. Effect of electrocrystallization medium on quality, structural features, and conducting properties of single crystals of the $(BEDT\text{-}TTF)_4A^I[Fe^{III}(C_2O_4)_3]\cdot G$ family. *CrystEngComm* **2011**, *13*, 537–545. [CrossRef]
20. Zorina, L.V.; Khasanov, S.S.; Simonov, S.V.; Shibaeva, R.P.; Zverev, V.N.; Canadell, E.; Prokhorova, T.G.; Yagubskii, E.B. Coexistence of two donor packing motifs in the stable molecular metal α-'pseudo-κ'-$(BEDT\text{-}TTF)_4(H_3O)[Fe(C_2O_4)_3]\cdot C_6H_4Br_2$. *CrystEngComm* **2011**, *13*, 2430–2438. [CrossRef]
21. Coronado, E.; Curreli, S.; Giménez-Saiz, C.; Gómez-García, C.J. The Series of Molecular Conductors and Superconductors $ET_4[AFe(C_2O_4)_3]\cdot PhX$ (ET = bis(ethylenedithio)tetrathiafulvalene; $(C_2O_4)^{2-}$ = oxalate; $A^+ = H_3O^+$, K^+; X = F, Cl, Br, and I): Influence of the Halobenzene Guest Molecules on the Crystal Structure and Superconducting Properties. *Inorg. Chem.* **2012**, *51*, 1111–1126. [PubMed]
22. Zorina, L.V.; Khasanov, S.S.; Simonov, S.V.; Shibaeva, R.P.; Bulanchuk, P.O.; Zverev, V.N.; Canadell, E.; Prokhorova, T.G.; Yagubskii, E.B. Structural phase transition in the β''-$(BEDT\text{-}TTF)_4H_3O[Fe(C_2O_4)_3]\cdot G$ crystals (where G is a guest solvent molecule). *CrystEngComm* **2012**, *14*, 460–465. [CrossRef]
23. Prokhorova, T.G.; Zorina, L.V.; Simonov, S.V.; Zverev, V.N.; Canadell, E.; Shibaeva, R.P.; Yagubskii, E.B. The first molecular superconductor based on BEDT-TTF radical cation salt with paramagnetic tris(oxalato)ruthenate anion. *CrystEngComm* **2013**, *15*, 7048–7055. [CrossRef]
24. Prokhorova, T.G.; Buravov, L.I.; Yagubskii, E.B.; Zorina, L.V.; Simonov, S.V.; Shibaeva, R.P.; Zverev, V.N. New metallic bi- and monolayered radical cation salts based on BEDT-TTF with tris(oxalato)gallate anion. *Eur. J. Inorg. Chem.* **2014**, *24*, 3933–3940. [CrossRef]
25. Prokhorova, T.G.; Buravov, L.I.; Yagubskii, E.B.; Zorina, L.V.; Simonov, S.V.; Zverev, V.N.; Shibaeva, R.P.; Canadell, E. Effect of Halopyridine Guest Molecules on the Structure and Superconducting Properties of β″-$[Bis(ethylenedithio)tetrathiafulvalene]_4(H_3O)[Fe(C_2O_4)_3]\cdot$Guest Crystals. *Eur. J. Inorg. Chem.* **2015**, *34*, 5611–5620. [CrossRef]
26. Martin, L.; Morritt, A.L.; Lopez, J.R.; Nakazawa, Y.; Akutsu, H.; Imajo, S.; Ihara, Y.; Zhang, B.; Zhange, Y.; Guof, Y. Molecular conductors from bis(ethylenedithio)tetrathiafulvalene with tris(oxalato)rhodate. *Dalton Trans.* **2017**, *46*, 9542–9548. [CrossRef] [PubMed]
27. Prokhorova, T.G.; Yagubskii, E.B. Organic conductors and superconductors based on bis(ethylenedithio)tetrathiafulvalene radical cation salts with supramolecular tris(oxalato)metallate anions. *Russ. Chem. Rev.* **2017**, *86*, 164–180. [CrossRef]

28. Coronado, E.; Galan-Mascaros, J.R.; Gomez-Garcia, C.J.; Laukhin, V. Coexistence of ferromagnetism and metallic conductivity in a molecule-based layered compound. *Nature* **2000**, *408*, 447–449. [CrossRef] [PubMed]
29. Martin, L.; Day, P.; Horton, P.; Nakatsuji, S.; Yamada, J.; Akutsu, H. Chiral conducting salts of BEDT-TTF containing a single enantiomer of tris(oxalato)chromate(III) crystallized from a chiral solvent. *J. Mater. Chem.* **2010**, *20*, 2738–2742. [CrossRef]
30. Martin, L.; Day, P.; Nakatsuji, S.; Yamada, J.; Akutsu, H.; Horton, P. A molecular charge transfer salt of BEDT-TTF containing a single enantiomer of tris(oxalato)chromate(III) crystallized from a chiral solvent. *CrystEngComm* **2010**, *12*, 1369–1372. [CrossRef]
31. Martin, L.; Akutsu, H.; Hortond, P.N.; Hursthoused, M.B. Chirality in charge-transfer salts of BEDT-TTF of tris(oxalato)chromate (III). *CrystEngComm* **2015**, *17*, 2783–2790. [CrossRef]
32. Martin, L.; Akutsu, H.; Horton, P.N.; Hursthouse, M.B.; Harrington, R.W.; Clegg, W. Chiral Radical-Cation Salts of BEDT-TTF Containing a Single Enantiomer of Tris(oxalato)aluminate(III) and -chromate(III). *Eur. J. Inorg. Chem.* **2015**, *11*, 1865–1870.
33. Martin, L.; Morritt, A.L.; Lopez, J.R.; Akutsu, H.; Nakazawa, Y.; Imajo, S.; Ihara, Y. Ambient-pressure molecular superconductor with a superlattice containing layers of tris(oxalato)rhodate enantiomers and 18-crown-6. *Inorg. Chem.* **2017**, *56*, 717–720. [CrossRef] [PubMed]
34. Mori, T. Structural Genealogy of BEDT-TTF-Based Organic Conductors I. Parallel Molecules: β and β'' Phases. *Bull. Chem. Soc. Jpn.* **1998**, *71*, 2509–2526. [CrossRef]
35. Mori, T.; Mori, H.; Tanaka, S. Structural Genealogy of BEDT-TTF-Based Organic Conductors II. Inclined Molecules: θ, α, and κ Phases. *Bull. Chem. Soc. Jpn.* **1999**, *72*, 179–197. [CrossRef]
36. Olejniczak, I.; Frackowiak, A.; Swietlik, R.; Prokhorova, T.G.; Yagubskii, E.B. Charge Fluctuations and Ethylene-Group-Ordering Transition in β''-(BEDT-TF)$_4$[(H$_3$O)Fe(C$_2$O$_4$)$_3$]·Y Molecular Charge-Transfer Salts. *ChemPhysChem* **2013**, *14*, 3925–3935. [CrossRef] [PubMed]
37. Neogi, P.; Dutt, N.K.J. New compounds of gallium. Part III. Preparation and Resolution of complex oxalate compounds of gallium into optical isomers. *Indian Chem. Soc.* **1938**, *15*, 83–86.
38. *CrysAlisPro Software System*, Version 1.171.38.41; Rigaku Oxford Diffraction; Rigaku Corporation: Oxford, UK, 2016.
39. Sheldrick, G.M. A short history of SHELX. *Acta Cryst. A* **2008**, *64*, 112–122. [CrossRef] [PubMed]
40. Guionneau, P.; Kepert, C.J.; Bravic, G.; Chasseau, D.; Truter, M.R.; Kurmoo, M.; Day, P. Determining the charge distribution in BEDT-TTF salts. *Synth. Met.* **1997**, *86*, 1973–1974. [CrossRef]
41. Martin, L.; Engelkamp, H.; Akutsu, H.; Nakatsuji, S.; Yamada, J.; Horton, P.; Hursthouse, M.B. Charge transfer salts of BEDT-TTF with lithium tris(oxalato)metallate(III). *Dalton Trans.* **2015**, *44*, 6219–6223. [CrossRef] [PubMed]
42. Zhang, B.; Zhang, Y.; Liu, F.; Guo, Y. Synthesis, crystal structure, and characterization of charge-transfer salt: (BEDT-TTF)$_5$[Fe(C$_2$O$_4$)$_3$]·(H$_2$O)$_2$·CH$_2$Cl$_2$ (BEDT-TTF = bis(ethylenedithio)tetrathiafulvalene). *CrystEngComm* **2009**, *11*, 2523–2528. [CrossRef]
43. Altshuler, B.L.; Aronov, A.G. Electron-Electron Interaction in Disordered Conductors. In *Electron-Electron Interactions in Disordered Systems*; Efros, A.L., Pollak, M., Eds.; Elsevier: Amsterdam, The Netherlands, 1985; Volume 10, pp. 1–690. ISBN 0444-86916-6.
44. Gruner, G.; Zawadowski, A. Magnetic impurities in non-magnetic metals. *Rep. Prog. Phys.* **1974**, *37*, 1497–1584. [CrossRef]